Chiral Switches

DOI: 10.1002/anie.201411313

Predicting the Switchable Screw Sense in Fluorene-Based Polymers**

Adriana Pietropaolo, Yue Wang, and Tamaki Nakano**

Abstract: *A chirality-switching free-energy landscape was reconstructed on a 43-mer of poly(9,9-dioctylfluoren-2,7-diyl) (PDOF). The simulations were conducted on amorphous silica surface as well as in the vacuum phase for a single chain or for a group of sixteen chains. The achiral-to-chiral transition occurs only on amorphous silica (activation free-energy 35 kcal mol^{-1}), where the enantiomeric (homochiral) basins are detected. This was supported by the experiments where effective chirality induction to PDOF using circularly polarized light (CPL) was attained only for a film deposited on a quartz glass and not for a solution or a suspension. These results indicate that interactions of PDOF with amorphous silica play a crucial role in chirality switching. Importance of chain assembling was also indicated. Theoretical ECD spectra of the enantiomeric basins containing a 5_1 helix reproduce the experimental spectra.*

Artificial chiral polymers lead to a wide variety of potential applications.[1] Some polymers can switch their chirality in a controlled manner by chemical[1e,2] and light[3,4] stimuli. We recently reported that optically inactive poly(9,9-dioctylfluoren-2,7-diyl) (PDOF) turned into an optically active conformation with switchable screw-sense where CPL was the only source of chirality.[3a] Polyfluorene derivatives are of wide interest in the field of organic electronics,[5,6] and the photo-induced chirality switching of PDOF may be applied for modulation of photoelectronic properties. CPL has been used for asymmetric syntheses and chirality switching of small molecules.[7–9] Although understanding and predicting helical sense switching in macromolecules are important issues for the bottom-up design of functional nanostructures,[10] the molecular mechanism of chirality induction and chirality switching of PDOF has not yet been clarified.

[*] Dr. A. Pietropaolo
Dipartimento di Scienze della Salute
Università di Catanzaro
Viale Europa, 88100 Catanzaro (Italy)
E-mail: apietropaolo@unicz.it
Y. Wang, Prof. Dr. T. Nakano
Catalysis Research Center (CRC)
Hokkaido University, N 21, W 10
Kita-ku, Sapporo 001-0021 (Japan)
E-mail: tamaki.nakano@cat.hokudai.ac.jp
Homepage: http://polymer.cat.hokudai.ac.jp/index-e.html

[**] PRACE Research Infrastructure resources support the results achieved on the FERMI machine based in Italy. ISCRA resources also support additional free-energy simulations and TDDFT calculations. The Catalysis Research Center (CRC), Hokkaido University—Overseas Research Fellow, 2013—is gratefully acknowledged for financial support.

Supporting information for this article is available on the WWW under http://dx.doi.org/10.1002/anie.201411313.

Herein, we present the mechanism of chirality induction in an achiral PDOF 43-mer by reconstructing the free-energy landscape through well-tempered[11] metadynamics[12] simulations. Spearhead contributions through molecular simulations[13–17] have been devoted on rationalizing the supramolecular structure and functions of self-assembled polyfluorenes.[15–17] However, the estimation of activation barriers in chirality switching has been hardly achieved owing to bottlenecks in their free-energy minima.[18] Atomistic simulations combined with free-energy estimates have been successfully exploited to reach a quantitative structural and energetic level of theory.[19]

In this study, free-energy landscapes of the PDOF 43-mer were obtained in four states, that is, a) a group of sixteen chains on amorphous silica, b) an isolated single chain on amorphous silica, c) a group of sixteen chains in vacuum, and d) an isolated, single chain in vacuum. The amorphous silica models were employed because a thin film sample deposited on a quartz glass substrate was used for chirality-switching experiments.[3a]

Free-energy simulations have been performed for these models through the combination of path-collective variables[20] and chirality index descriptors,[21] which are used as reaction coordinates.[22]

The free-energy landscape was reconstructed along the chiral path through the s_G and z_G coordinates. The first coordinate (s_G) identifies the reactive chiral path, from the 100% negatively-twisted ($s_G = -1$) to the 100% positively-twisted conformations ($s_G = +1$), crossing the racemic states ($s_G = 0$), and it reflects switching of the fluorene–fluorene dihedral angles. The latter coordinate (z_G) identifies instead the distance from an endowed path, in terms of fluxionality in the octyl side chains, and it reflects the side chain conformation as well as the different self-assembled forms.

Scheme 1 depicts a reference chiral path with eight frames equally spaced in chirality metrics including the 25%, 50%, 75%, and 100% negatively-twisted conformations, as well as the relative positively twisted conformations.

The racemic states are interpolated in between the 25% negatively and 25% positively twisted conformations. In this way, each of the frames represents a stepwise event in the chirality induction mechanism.

The free-energy landscape for sixteen PDOF chains on amorphous silica points to the presence of two enantiomeric deep minima centered at $s_G = -1$ and $s_G = +1$, $z_G = 0.3$ where neighboring chains are closely assembled (Figure 1 a).

These two free-energy basins have comparable stability. Furthermore, two racemic minima were found at $s_G = 0$, $z_G = 0.6$ and at $s_G = 0$, $z_G = 0.3$ where chain assembling is less close compared to that in the enantiomeric minima. The two racemic minima are separated by an activation free-energy of 35 kcal mol^{-1}, which cannot be readily overcome by thermal stimuli at room temperature but by photoirradiation.

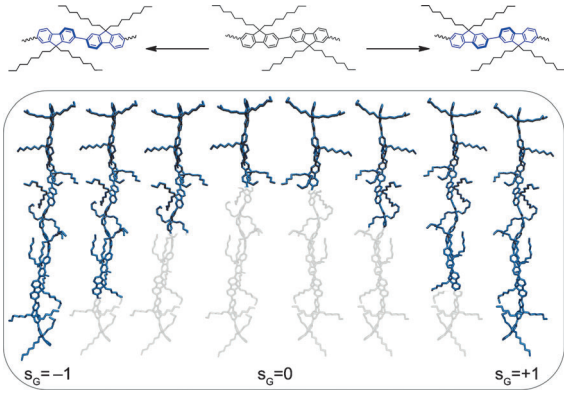

Scheme 1. Stepwise chirality switching on racemic PDOF ($s_G = 0$, $z_G \geq 0$) to positively twisted ($s_G = +1$, $z_G \geq 0$) and negatively twisted ($s_G = -1$, $z_G \geq 0$) conformations. A sketch of a PDOF section containing a 5_1 helix is taken here as a reference frame for visual purposes only. Racemic sections are shown in gray; the chiral sections are shown in blue.

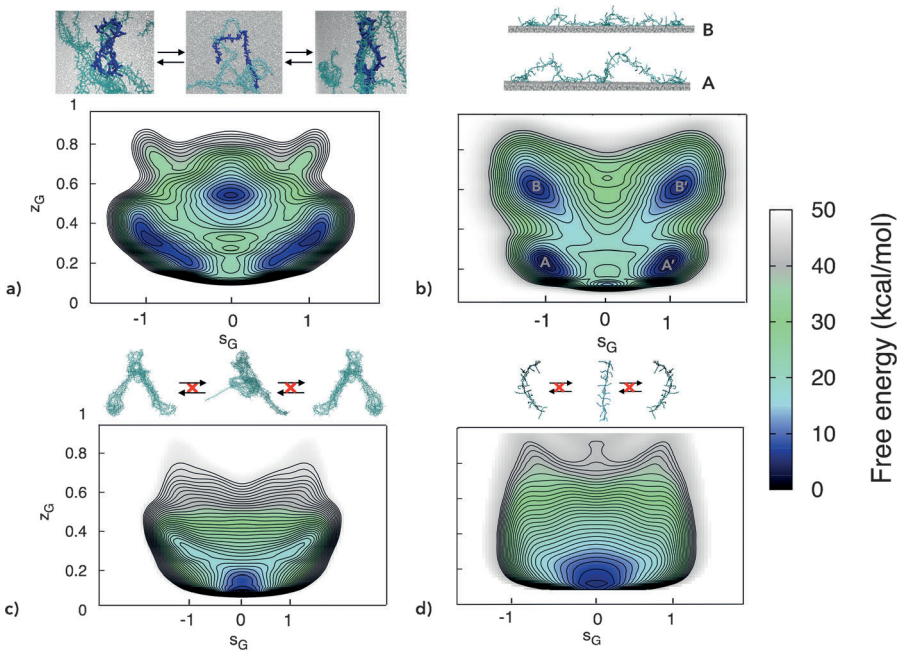

Figure 1. Free-energy profiles of the achiral-to-chiral transition of PDOF. a) Sixteen chains of PDOF deposited on amorphous silica (top: chain models corresponding to the chiral switch cycle), b) one chain of PDOF deposited on amorphous silica (top: the anchoring of PDOF on amorphous silica (A and B), c) sixteen chains of PDOF in vacuum, and d) one chain of PDOF in vacuum. In (a), where the chiral cycle can occur, the free-energy basins in the main panel correspond to the models shown in deep blue. A picture of the forbidden transition is also shown in (c) and (d).

The enantiomeric basins show portions of 5_1 left- and right-handed helical conformations. Those are characterized by a dihedral angle of fluorene–fluorene diad ranging from 45 to 72 degrees (Supporting Information, Figure S1a). Similar angles have been reported for the 5_1 helix conformation.[15e]

In contrast, in the racemic basin, the PDOF chains take mores stretched conformations, with kinks often connecting right- and left-handed helical sections. The first deeper and the second shallower racemic basins indicate a largely kinked and a rather elongated conformation, respectively. Intriguingly, the enantiomeric minima show a deep funnel shape indicating that once the first five fluorene–fluorene dihedral angles are twisted, chirality amplification starts along the chain. CPL triggers a stepwise fluorene–fluorene twist at the chain termini, propagating along the chain following the sergeants and soldiers effects.[23] In these regards, the chiral amplification in the PDOF case may be related to the chirality induction systems with small chiral molecules.[24]

As shown in Figure 1b, when only one PDOF chain is deposited on amorphous silica, two sets of enantiomeric minima were found at $s_G = -1$, $s_G = +1$ and $z_G = 0.2$ and $z_G = 0.6$ (highlighted as A and B and A′ and B′), along with a rather deep racemic minimum at $s_G = 0$ and $z_G = 0.1$, which is less stable in free energy by $+10$ kcal mol^{-1} than the enantiomeric minima. The free-energy barrier between A or B and the racemic basin is still about 35 kcal mol^{-1}. These results indicate that, even without chain-to-chain interaction, chirality induction is feasible for single chain interacting with silica. However, compared with the situation in Figure 1a where chain-to-chain interaction can occur, once a chain reaches an enantiomeric basin, it shows an increased stability with respect to the racemic states (Figure 1b), hampering a smooth chirality switching.

As for enantiomeric minima, A and B (A′ and B′) represent two distinct binding modes of PDOF on the amorphous silica. The first minimum is connected to a partial 15_1 helix (A), while the second one is related to sections of a 5_1 helix (B) where the latter chain seems to interact with silica more closely. The interaction between PDOF and amorphous silica is most probably based on van der Waals forces; however, the weak force seems to be very important in stabilizing a chiral structure of PDOF.

The results obtained so far indicate that self-assembling of PDOF and interaction of PDOF with support are essential for the chirality switching. To clarify how the self-assembling can affect the chirality induction in the absence of silica, we reconstructed the free-energy landscape for a group of sixteen PDOF chains in the vacuum phase. Intriguingly, the free-energy landscape reported in Figure 1c indicates the presence of one broad, deep central (racemic) minima, centered at values of $s_G = 0$, $z_G = 0.1$, with two rather shallow enantiomeric minima at $s_G = -1$, $s_G = +1$, and $z_G = 0.3$. Because the enatiomeric minima are much less stable than the racemic basin, they would let the polymer go back to the racemic state.

The chains in vacuum are more closely aggregated both in the racemic and enantiomeric states compared with chains deposited on amorphous silica and they appear rather stretched (rather zigzag planar-like), facilitating aggregation through π–π stacking.

The former elongated conformations are further supported through the adoption of relatively large torsional twists in the PDOF aggregated states (Supporting Information, Figure S2a), as also observed in the amorphous aggregated states of PDOF.[17]

Furthermore, the free-energy landscape of a single chain in the vacuum phase was rather similar to that of a group of sixteen chains noted above (Figure 1 d). It has one broad minimum with no clear minima corresponding to enantiomeric states where chirality induction would be difficult. The racemic basin in vacuum identifies a "spaghetti-like" structure that is almost zigzag planar.

These results strongly suggest that chirality switching would be difficult regardless of how chains are assembled in the absence of silica and that PDOF–support interaction plays a crucial role in chirality induction. This aspect was assessed by experiments. We attempted to induce chirality of a suspension of PDOF (M_n 99500, M_w/M_n 2.36 vs. polystyrene standard) in a toluene–MeOH mixture (5:1, *v*/*v*) using CPL from an Hg-Xe lamp and found that maximum anisotropy in circular dichroism (CD) spectra achieved by chirality of light was far smaller in suspension (Kuhn's anisotropy factor (g_{CD} in the order of 10^{-5}; Supporting Information, Figure S7) than in film deposited on a quartz glass plate (g_{CD} in the order of 10^{-3}; Supporting Information, Figure S7). Thus, solid substrate such as amorphous silica seems to be indispensable in effectively inducing and switching chirality of PDOF by CPL. The solid support acts as a scaffold, allowing a smooth chirality induction and preventing an uncontrolled stacking among the PDOF chains. In this regard, it is known that a strong π–π stacking inhibits a helical conformation.[16a]

Chirality induction to PDOF in a dilute solution was not possible.[3a] This supports the simulation result that single-chain chirality switching would be difficult, as predicted from the free-energy landscape reported in Figure 1 d.

It should be noted here that high g_{CD} values (10^{-3} order) were achieved without a solid support for poly[(9,9-di-noctylfluorenyl-2,7-diyl)-alt-4,4′-azo-benzene][3b] by CPL and for poly(9,9-di-*n*-decylfluorene)[25] through interactions with chiral small molecules. Thus, the chirality induction mechanism may vary depending on chemical structure of a polymer and on the interacting substrate.

We assessed the accuracy of the proposed chirality switching mechanism by calculating the electronic UV spectra of 2,2′-difluorenyl as a dimer model at the TDDFT level through the B97-D functional[26] (Figure 2 a). This model is considered reasonable, as it may represent the shortest chiral sequence in PDOF, and CPL irradiation induces a change in the fluorene–fluorene dihedral angle.[3a]

In experiments, on inducing chirality to a PDOF film deposited on a quartz plate, UV spectra indicated overall blue-shifts and hypochromism (Figure 2 b). Intensities of the lower-energy bands at 430 nm and at 400 nm decreased with respect to those of the other bands, suggesting a transition

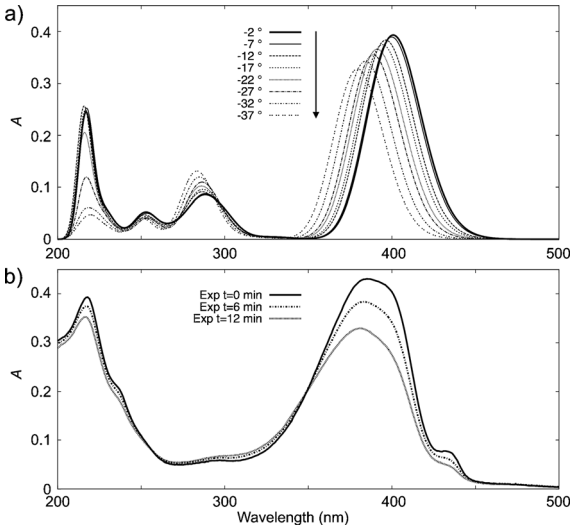

Figure 2. UV spectra calculated for 2,2′-difluorenyl as a function of the fluorene–fluorene dihedral angle (a) and experimental spectra observed on chirality induction (b).[3a] The value of −37° corresponds to the twist adopted in the 2,2′-difluorenyl ground state.

from a rather coplanar-like fluorene–fluorene confomation to a more twisted conformation. Although the calculated spectra did not reproduce the low-intensity band at 430 nm which disappear through CPL irradiation, overall blue-shifts and hypochromism were well-reproduced.

We then proceeded to calculate ECD spectra. As preliminary calculations on 2,2′-difluorenyl as a dimer model at the TDDFT level (Supporting Information, Figures S8, S9) did not reproduce the experimental spectral shapes well, the calculation was extended to a 10-mer model within the ZINDO[27] method (Figure 3), ensuring that changing from TDDFT to ZINDO the signs were not inverted and the overall shapes of the spectra were conserved (Supporting Information, Figures S8, S10).

Figure 3 shows the ECD spectra calculated for the negatively and positively twisted PDOF decamers corresponding to conformations containing 5_1 helix found in the enantiomeric basins in Figure 1 a. The calculated spectra are strikingly similar to the experimental spectra. These results clearly indicate that 5_1 helical structure which was found in the enantiomeric basins is the most probable conformation achieved during chirality induction by CPL.[3a] Thus, the free-energy landscapes obtained in this work can be concluded to be credible.

Moreover, the calculated ECD spectra indicate that the negatively twisted conformation of the 43-mer PDOF is afforded by the R-CPL irradiation, while the positively-twisted conformation originates from the L-CPL irradiation.

In conclusion, we have predicted and quantitatively rationalized the molecular basis of chirality switching of PDOF. We have devised a chiral path, thereby switching in a stepwise manner the fluorene–fluorene dihedral twist. The free-energy landscapes predict that chirality switching of the polyfluorene derivative is feasible only when it is deposited on amorphous silica. This observation was experimentally supported through the low and zero dichroic signals found,

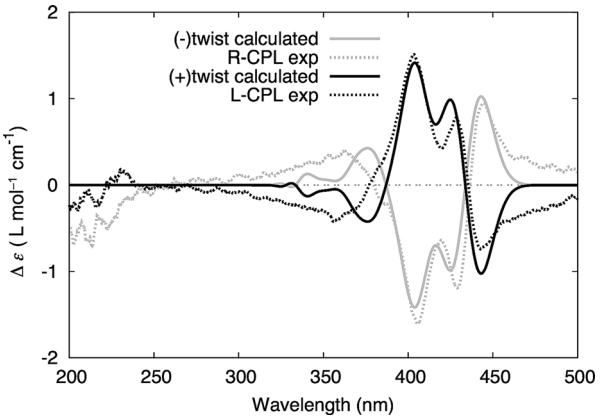

Figure 3. ECD spectra calculated at the ZINDO level for the negative (−) and positive (+) twist basins considering decamer sections of poly(fluoren-2,7-diyl) with the relating experimental spectra recorded after 6 min of CPL irradiation.

respectively, for a suspension and a solution of the polymer without quartz glass support. Solid substrate surface may facilitate the achiral-to-chiral transition as an inert supramolecular scaffold.

Received: November 21, 2014
Revised: December 9, 2014
Published online: January 13, 2015

Keywords: chiral switches · chirality induction · helical structures · molecular dynamics · polymers

[1] a) Y. Okamoto, K. Hatada, *J. Liq. Chromatogr.* **1986**, *9*, 369 – 384; b) T. Nakano, *J. Chromatogr. A* **2001**, *906*, 205 – 225; c) Y. Okamoto, *J. Polym. Sci. Part A* **2009**, *47*, 1731 – 1739; d) Y. Okamoto, T. Nakano, *Chem. Rev.* **1994**, *94*, 349 – 372; e) T. Nakano, Y. Okamoto, *Chem. Rev.* **2001**, *101*, 4013 – 4038; f) E. Yashima, K. Maeda, H. Iida, Y. Furusho, K. Nagai, *Chem. Rev.* **2009**, *109*, 6102 – 6211.

[2] a) E. Yashima, K. Maeda, Y. Okamoto, *Nature* **1999**, *399*, 449 – 451; b) Y. Okamoto, H. Mohri, T. Nakano, K. Hatada, *J. Am. Chem. Soc.* **1989**, *111*, 5952 – 5954; c) T. Yamamoto, T. Yamada, Y. Nagata, M. Suginome, *J. Am. Chem. Soc.* **2010**, *132*, 7899 – 7901.

[3] a) Y. Wang, T. Sakamoto, T. Nakano, *Chem. Commun.* **2012**, *48*, 1871 – 1873; b) M. Fujiki, K. Yoshida, N. Suzuki, J. Zhang, W. Zhang, X. Zhu, *RSC Adv.* **2013**, *3*, 5213 – 5219; c) J. Li, G. B. Schuster, K.-S. Cheon, M. M. Green, J. V. Selinger, *J. Am. Chem. Soc.* **2000**, *122*, 2603 – 2612; d) T. Sakamoto, Y. Fukuda, S. Sato, T. Nakano, *Angew. Chem. Int. Ed.* **2009**, *48*, 9308 – 9311; *Angew. Chem.* **2009**, *121*, 9472 – 9475; e) L. Nikolova, T. Todorov, M. Ivanov, F. Andruzzi, S. Hvilsted, P. S. Ramanujam, *Opt. Mater.* **1997**, *8*, 255 – 258; f) G. Iftime, F. L. Labarthet, A. Natansohn, P. Rochon, *J. Am. Chem. Soc.* **2000**, *122*, 12646 – 12650; g) A. Natansohn, P. Rochon, *Adv. Mater.* **1999**, *11*, 1387 – 1391.

[4] T. Nakano, *Chem. Rec.* **2014**, *14*, 369 – 385.

[5] a) A. C. Grimsdale, K. L. Chan, R. E. Martin, P. G. Jokisz, A. B. Holmes, *Chem. Rev.* **2009**, *109*, 897 – 1091; b) N. Martino, D. Fazzi, C. Sciascia, A. Luzio, M. R. Antognazza, M. Caironi, *ACS Nano* **2014**, *8*, 5968 – 5978; L. Angiolini, T. Benelli, L. Giorgini, A. Golemme, F. Mauriello, E. Salatelli, R. Termine, *Macromol. Chem. Phys.* **2008**, *209*, 944 – 956.

[6] A. Saywell, J. Schwarz, S. Hecht, L. Grill, *Angew. Chem. Int. Ed.* **2012**, *51*, 5096 – 5100; *Angew. Chem.* **2012**, *124*, 5186 – 5190.

[7] a) J. A. Le Bell, *Bull. Soc. Chim. Fr.* **1874**, *22*, 337 – 347; b) J. H. Van't Hoff, Pamphlet, September 3, **1874**, Utrecht.

[8] a) Y. Inoue, *Chem. Rev.* **1992**, *92*, 741 – 770; b) B. L. Feringa, R. A. Delden, *Angew. Chem. Int. Ed.* **1999**, *38*, 3418 – 3438; *Angew. Chem.* **1999**, *111*, 3624 – 3645.

[9] a) T. Kawasaki, M. Sato, S. Ishiguro, T. Saito, Y. Morishita, I. Sato, H. Nishino, Y. Inoue, K. Soai, *J. Am. Chem. Soc.* **2005**, *127*, 3274 – 3275; b) K. Soai, T. Shibata, H. Morioka, K. Choji, *Nature* **1995**, *378*, 767 – 768; c) N. P. M. Huck, W. F. Jager, B. deLange, B. L. Feringa, *Science* **1996**, *273*, 1686 – 1688; d) B. L. Feringa, N. P. M. Huck, A. M. Schoevaars, *Adv. Mater.* **1996**, *8*, 681 – 684.

[10] A. C. Grimsdale, K. Müllen, *Angew. Chem. Int. Ed.* **2005**, *44*, 5592 – 5629; *Angew. Chem.* **2005**, *117*, 5732 – 5772

[11] A. Barducci, G. Bussi, M. Parrinello, *Phys. Rev. Lett.* **2008**, *100*, 020603.

[12] A. Laio, M. Parrinello, *Proc. Natl. Acad. Sci. USA* **2002**, *99*, 12562 – 12566.

[13] a) P. Leclère, E. Hennebicq, A. Calderone, P. Brocorens, A. C. Grimsdale, K. Müllen, J. L. Brédas, R. Lazzaroni, *Prog. Polym. Sci.* **2003**, *28*, 55 – 81; b) P. Leclère, M. Surin, P. Jonkheijm, O. Henze, A. P. H. J. Schenning, F. Biscarini, A. C. Grimsdale, W. J. Feast, E. W. Meijer, K. Müllen, J. L. Brédas, R. Lazzaroni, *Eur. Polym. J.* **2004**, *40*, 885 – 892; c) M. Linares, A. Minoia, P. Brocorens, D. Beljonne, R. Lazzaroni, *Chem. Soc. Rev.* **2009**, *38*, 806 – 816.

[14] a) J. Cornil, S. Verlaak, N. Martinelli, A. Mityashin, Y. Olivier, T. Van Regemorter, G. D'Avino, L. Muccioli, C. Zannoni, F. Castet, D. Beljonne, P. Heremans, *Acc. Chem. Res.* **2013**, *46*, 434 – 443; b) L. Muccioli, G. D'Avino, R. Berardi, S. Orlandi, A. Pizzirusso, M. Ricci, O. M. Roscioni, C. Zannoni, *Top. Curr. Chem.* **2014**, *352*, 39 – 101; c) T. Körzdörfer, J. L. Brédas, *Acc. Chem. Res.* **2014**, *47*, 3284 – 3291.

[15] a) G. Lieser, M. Oda, T. Miteva, A. Meisel, H.-G. Nothofer, U. Scherf, *Macromolecules* **2000**, *33*, 4490 – 4495; b) W. Chunwaschirasiri, B. Tanto, D. L. Huber, M. J. Winokur, *Phys. Rev. Lett.* **2005**, *94*, 107402; c) C. Chi, G. Lieser, V. Enkelmann, G. Wegner, *Macromol. Chem. Phys.* **2005**, *206*, 1597 – 1609; d) V. Marcon, N. van der Vegt, G. Wegner, G. Raos, *J. Phys. Chem. B* **2006**, *110*, 5253 – 5261; e) M. Oda, H.-G. Nothofer, U. Scherf, V. Sunjic, D. Richter, W. Regenstein, D. Neher, *Macromolecules* **2002**, *35*, 6792 – 6798.

[16] a) M. Knaapila, R. Stepanyan, B. P. Lyons, M. Torkkeli, A. P. Monkman, *Adv. Funct. Mater.* **2006**, *16*, 599 – 609; b) M. J. Winokur, J. Slinker, D. L. Huber, *Phys. Rev. B* **2003**, *67*, 184106.

[17] S. Kilina, E. R. Batista, P. Yang, S. Tretiak, A. Saxena, R. L. Martin, D. L. Smith, *ACS Nano* **2008**, *2*, 1381 – 1388.

[18] A. Pietropaolo, T. Nakano, *J. Am. Chem. Soc.* **2013**, *135*, 5509 – 5512.

[19] a) W. F. van Gunsteren, D. Bakowies, R. Baron, I. Chandrasekhar, M. Christen, X. Daura, P. Gee, D. P. Geerke, A. Glättli, P. H. Hünenberger, M. A. Kastenholz, C. Oostenbrink, M. Schenk, D. Trzesniak, N. F. van der Vegt, H. B. Yu, *Angew. Chem. Int. Ed.* **2006**, *45*, 4064 – 4092; *Angew. Chem.* **2006**, *118*, 4168 – 4198; b) D. J. Wales, P. Salamon, *Proc. Natl. Acad. Sci. USA* **2014**, *111*, 617 – 622.

[20] D. Branduardi, F. L. Gervasio, M. Parrinello, *J. Chem. Phys.* **2007**, *126*, 054103.

[21] a) M. A. Osipov, B. T. Pickup, D. A. Dunmur, *Mol. Phys.* **1995**, *84*, 1193 – 1206; b) M. Solymosi, R. J. Low, M. Grayson, M. P. Neal, *J. Chem. Phys.* **2002**, *116*, 9875 – 9881; c) A. Pietropaolo, L. Muccioli, R. Berardi, C. Zannoni, *Proteins Struct. Funct. Bioinf.* **2008**, *70*, 667 – 677; d) A. Pietropaolo, M. Parrinello, *Chirality* **2011**, *23*, 534 – 542.

[22] A. Pietropaolo, D. Branduardi, M. Bonomi, M. Parrinello, *J. Comput. Chem.* **2011**, *32*, 2627 – 2637.

[23] M. M. Green, M. P. Reidy, R. J. Johnson, G. Darling, D. J. Oleary, G. Willson, *J. Am. Chem. Soc.* **1989**, *111*, 6452 – 6454.
[24] a) W. Makiguchi, S. Kobayashi, Y. Furusho, E. Yashima, *Angew. Chem. Int. Ed.* **2013**, *52*, 5275 – 5279; *Angew. Chem.* **2013**, *125*, 5383 – 5387; b) K. Shimomura, T. Ikai, S. Kanoh, E. Yashima, K. Maeda, *Nat. Chem.* **2014**, *6*, 429 – 434.
[25] Y. Nakano, Y. Liu, M. Fujiki, *Polym. Chem.* **2010**, *1*, 460 – 469.
[26] S. Grimme, *J. Comput. Chem.* **2006**, *27*, 1787 – 1799.
[27] a) J. Ridley, M. C. Zerner, *Theor. Chim. Acta* **1973**, *32*, 111 – 134; b) J. Ridley, M. C. Zerner, *J. Mol. Spectrosc.* **1974**, *50*, 457 – 473.

